Accepted Manuscript

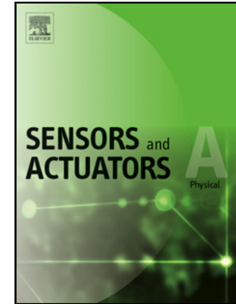

Title: An Experimental and Theoretical Investigation of Electrostatically Coupled Cantilever Microbeams

Author: Saad Ilyas Karumbaiah N. Chappanda<ce:author id="aut0015" biographyid="vt0015" orcid="0000-0002-1257-5093"> Md A. Al Hafiz Abdallah Ramini Mohammad I. Younis

PII: S0924-4247(16)30307-7
DOI: http://dx.doi.org/doi:10.1016/j.sna.2016.06.021
Reference: SNA 9723

To appear in: *Sensors and Actuators A*

Received date: 10-2-2016
Revised date: 24-3-2016
Accepted date: 15-6-2016

Please cite this article as: Saad Ilyas, Karumbaiah N.Chappanda, Md A.Al Hafiz, Abdallah Ramini, Mohammad I.Younis, An Experimental and Theoretical Investigation of Electrostatically Coupled Cantilever Microbeams, Sensors and Actuators: A Physical http://dx.doi.org/10.1016/j.sna.2016.06.021

This is a PDF file of an unedited manuscript that has been accepted for publication. As a service to our customers we are providing this early version of the manuscript. The manuscript will undergo copyediting, typesetting, and review of the resulting proof before it is published in its final form. Please note that during the production process errors may be discovered which could affect the content, and all legal disclaimers that apply to the journal pertain.

ACCEPTED MANUSCRIPT

An Experimental and Theoretical Investigation of Electrostatically Coupled Cantilever Microbeams

Saad Ilyas, Karumbaiah N. Chappanda, Md A. Al Hafiz, Abdallah Ramini, Mohammad I. Younis

Physical Sciences and Engineering (PSE), King Abdullah University of Science and Technology, 23955-6900 Thuwal, KSA
mohammad.younis@kaust.edu.sa.

ACCEPTED MANUSCRIPT

Highlights

- We present an experimental and theoretical investigation of the static and dynamic behavior of electrostatically coupled laterally actuated silicon microbeams.
- The theoretical model is developed using the distributed parameter approach.
- The dual beam resonators are demonstrated as a way to reduce the pull-in voltage as well as pull-in time by more than 30% as compared to the case of individual beam actuation against the fixed electrode. A closed form for pull-in voltage has also been developed.
- The dynamics of the dual beam resonators show that we can control the coupling between the resonators by manipulating the DC voltage. Modeshape coupling has been demonstrated using finite element analysis. Electrostatically coupled dual beam resonators, are also proposed as a way to increase bandwidth near the natural frequency of the beam.
- Finally, dynamic pull-in of the coupled system is studied and proposed as sensor capable of sensing both a positive or negative shift in the frequency.

***Abstract*—We present an experimental and theoretical investigation of the static and dynamic behavior of electrostatically coupled laterally actuated silicon microbeams. The coupled beam resonators are composed of two almost identical flexible cantilever beams forming the two sides of a capacitor. The experimental and theoretical analysis of the coupled system is carried out and compared against the results of beams actuated with fixed electrodes individually. The pull-in characteristics of the electrostatically coupled beams are studied, including the pull-in time. The dynamics of the coupled dual beams are explored via frequency sweeps around the neighborhood of the natural frequencies of the system for different input voltages. Good agreement is reported among the simulation results and the experimental data. The results show considerable drop in the pull-in values as compared to single microbeam resonators. The dynamics of the coupled beam resonators are demonstrated as a way to increase the bandwidth of the resonator near primary resonance as well as a way to introduce increased frequency shift, which can be promising for resonant sensing applications. Moreover the dynamic pull-in characteristics are also studied and proposed as a way to sense the shift in resonance frequency.**

***Index Terms*—Micro cantilevers, Static pull-in, Pull-in time, Coupled resonators, Electrostatic actuation, Bandwidth, Dynamic pull-in**

1. Introduction

The interesting static and dynamic behavior of MEMS structures has drawn significant attention in the MEMS community in the last two decades. Microbeams, such as cantilevers and clamped-clamped beams, have been explored in great detail and are being used in variety of applications, especially in sensing [1-3] and wireless communication [4-5]. Moreover, initially curved or arched beams have been also explored due to their powerful dynamic characteristics and have been proposed as mechanical filters [6]. Other kinds of resonators, such as MEMS torsional resonators, have been proposed for applications in bandwidth tunability [7], thermal sensing [8], and logic operations [9]. The static and dynamic features of these structures become more complex when coupled and interacting with each other. It is necessary to understand the mechanical behaviors in such cases in order to exploit them efficiently or avoid them, when necessary.

Considerable efforts have been directed towards understanding the complex static and dynamic behavior of coupled MEMS resonators. The method of multiple scales combined with a reduced order model has been explored for a system of two electrostatically coupled parallel identical micro cantilevers and a ground plate [10]. A detailed study of the natural frequencies and mode shapes of mechanically coupled microbeam resonators with an application to MEMS filters has been reported in [11]. Moreover, a detailed characterization of mechanically and electrostatically coupled micro cantilevers has been demonstrated in [12]. The study in [12] deals with out-of-plane cantilevers, mechanically coupled at the common base, placed very close to each other. This proximity induces coupling in the device dynamics, which has been modeled and verified experimentally.

ACCEPTED MANUSCRIPT

Electromechanical coupling is commonly used in mixer and filters applications. The coupling beam concept is well known in RF filters, where it is used as a medium to transfer energy from one resonator to another [13, 14]. A high-Q filter composed of two doubly clamped microbeams mechanically coupled by a soft flexural-mode mechanical spring has been reported in [15]. A detailed study on electrically coupled MEMS bandpass filters has been reported in [16, 17]. The study in [16] demonstrates the concept of passive coupling of resonators using capacitors as the coupling element for filter synthesis. It also introduces and demonstrates the concept of active coupling of resonators using transistor-based amplifying circuits. The study in [17] presents the electrostatic coupling of closely spaced micro resonators without using a distinct coupling element. Vertical coupling in MEMS resonators has been demonstrated for the first time in [18]. The study demonstrates two mechanically coupled MEMS plates for phase noise reduction. Arrays of coupled oscillators have also been used to a great advantage. A novel filter scheme combining both electrical and mechanical coupling mechanisms using an array of microbeams has been reported in [19]. The study in [19] demonstrates an arrow percent bandwidth through a weak mechanical coupling and a decent stop band rejection via the electrical coupling. Arrays of mechanically coupled two-port CMOS-MEMS free-free microbeams have been demonstrated in [20]. These arrays have been shown to improve power handling capabilities; hence paving the way to realize low-phase-noise CMOS-MEMS oscillators in the future. Moreover, thermal coupling of an electrostatically actuated microbeam resonator has also been explored in [21]. One can note from the above that understanding the mechanical behavior of coupled systems is necessary to enable successful exploitation of them in sensing and actuation applications.

Another area of exploration in the MEMS community has been to develop low voltage switches [22-26]. These switches are used in various applications, such as MEMS logic/memory devices and RF applications. A design of an ohmic contact RF switch based on electrostatically coupled microbeams is presented in [22], where a theoretical reduced order model is developed to study the statics and dynamics of the system while discussing advantages of a single beam arrangement over a double beam configuration. A laterally actuated low voltage MEMS switch for high RF power is reported in [23], where they relied on thermal actuation to achieve low voltage switching. Similarly, a low voltage (~1 V_{pp}) complementary logic operation has been achieved by biasing of a parallel dual-beam piezo-based mechanical relays [24].

In this work we investigate the static and dynamic characteristics of electrostatically coupled micro cantilevers. The organization of the paper is as follows. In Section 2, we discuss the design and fabrication process of the laterally actuated and electrostatically coupled dual beam resonators. Next in Section 3, the mathematical model using a distributed parameter approach is discussed. Section 4 presents the experimental setup and procedures used in gathering the data. Section 5 presents different case studies performed in order to understand the static and dynamic behavior of the coupled beam resonators. Finally, Section 6 summarizes the results and presents conclusions.

2. Design and Fabrication

2.1. Design

The design of the device consists of two microbeams of the same width and thickness, but of slightly different lengths placed at a separating gap distance *d* between them, as shown in Fig. 1(a). Also, shown in Fig. 1(a) are the two fixed electrodes spanning the full lengths of the beams on each side. These electrodes are also separated by a distance *d* from the beams on either side. This arrangement allows for both of the beams to be separately actuated by applying potential difference among the beams and their respective electrodes (uncoupled). The beams can also be actuated by providing potential difference among themselves (coupled). It is worth mentioning here that the beams of slightly different lengths are chosen in order to realize two close but different frequencies of the system, which may lead to promising interaction among the modes, and hence can be potentially useful in practical applications.

2.2. Fabrication

The microbeams are fabricated by a two-mask process starting from a 4”double side polished, (100) oriented, p-doped and highly conductive (resistivity of 0.001 ohm.cm) SOI wafer consisting of 500µm Si handle layer, 2µm buried SiO_2 layer, and 25/30 µm Si device layer. The fabrication cross section of the beams is given in Fig. 2. First, a thin layer of Cr/Au (50/250 nm) is patterned and deposited on top forming the bond pads to provide input signals to

ACCEPTED MANUSCRIPT

the device via wire bonding/probing. Next, the silicon is patterned and etched defining the microbeam structures. Finally, the structures are released using HF vapor release to prevent stiction.

Fig. 3 shows an SEM image of the coupled beams. It can be noticed that both beams are aligned at their free ends. Fixed electrodes on each side of the beams for separate actuations are also shown. It can also be noticed that the beams are extended from the base by a small beam like structures. The dimensions of these extensions are very small and the structure itself is very rigid, hence the beams can be treated fixed at the anchors as in simple cantilevers. These extensions are introduced to keep the beam electrodes separate from each other in order to reduce parasitic capacitances. It is also noticed that there is no mechanical coupling among the two beams and the coupling comes solely from the electrostatic voltage (V_{DC}) applied between the two beams.

3. Modeling

The system of equations governing the motion of the coupled cantilevers, which are electrostatically actuated by a DC polarization voltage V_{DC}, and an AC harmonic load V_{AC} with a frequency Ω, can be written as

$$EIw_1''''(x_1,t)+\rho bh\ddot{w}_1(x_1,t)+c\dot{w}_1(x_1,t)=\frac{\varepsilon b\left[V_{DC}+V_{AC}\cos(\Omega t)\right]^2}{2(d-w_1+w_2)^2} \quad (1)$$

$$EIw_2''''(x_2,t)+\rho bh\ddot{w}_2(x_2,t)+c\dot{w}_2(x_2,t)=\frac{-\varepsilon b\left[V_{DC}+V_{AC}\cos(\Omega t)\right]^2}{2(d-w_1+w_2)^2} \quad (2)$$

where E is the modulus of elasticity, I is the moment of inertia, c is the damping coefficient, ρ is the density, ε is the air permittivity, d is the air gap between the two beams, b is the width of the beams, h is the thickness of the beams, t is time, x_1 is the position along beam 1, x_2 is the position along beam 2 , and w_1 and w_2 are the deflections of beam 1 and beam 2, respectively. The superscript "prime" indicates spatial derivative and the "dot" indicates temporal derivative.

The boundary conditions for the cantilever beams are

$$w_{1,2}(0,t)=0 \qquad \frac{\partial w_{1,2}}{\partial x_{1,2}}(0,t)=0$$

$$\frac{\partial^2 w_{1,2}}{\partial x_{1,2}^{\ 2}}(l_{1,2},t)=0 \qquad \frac{\partial^3 w_{1,2}}{\partial x_{1,2}^{\ 3}}(l_{1,2},t)=0 \quad (3)$$

Next, we introduce the following nondimensional variables, denoted by hats:

$$\hat{w}_1=\frac{w_1}{d};\qquad \hat{x}_1=\frac{x_1}{l_1};\qquad \hat{t}=\frac{t}{T};\qquad \hat{w}_2=\frac{w_2}{d};\qquad \hat{x}_2=\frac{x_2}{l_2} \quad (4)$$

Substituting (4) into (1) and (2) we get

$$\hat{w}_1''''+\frac{\rho bhl_1^{\ 4}}{EIT^2}\ddot{\hat{w}}_1+\frac{cl_1^{\ 4}}{EIT}\dot{\hat{w}}_1=\frac{\varepsilon bl_1^{\ 4}\left[V_{DC}+V_{AC}\cos(\Omega\hat{t}T)\right]^2}{2d^3EI(1-\hat{w}_1+\hat{w}_2)^2} \quad (5)$$

$$\hat{w}_2''''+\frac{\rho bhl_2^{\ 4}}{EIT^2}\ddot{\hat{w}}_2+\frac{cl_2^{\ 4}}{EIT}\dot{\hat{w}}_2=\frac{-\varepsilon bl_2^{\ 4}\left[V_{DC}+V_{AC}\cos(\Omega\hat{t}T)\right]^2}{2d^3EI(1-\hat{w}_1+\hat{w}_2)^2} \quad (6)$$

Next, we introduce the following parameters and drop the hats for convenience

$$\frac{\rho bhl_1^{\ 4}}{EIT^2}=1\Rightarrow T=\sqrt{\frac{\rho bhl_1^{\ 4}}{EI}};\qquad c_{non1}=\frac{cl_1^{\ 4}}{EIT};\qquad \alpha_1=\frac{\varepsilon bl_1^{\ 4}}{2d^3EI} \quad (7)$$

$$c_{non2}=\frac{cl_2^{\ 4}}{EIT};\qquad \alpha_2=\frac{\varepsilon bl_2^{\ 4}}{2d^3EI};\qquad \beta=\left(\frac{l_2}{l_1}\right)^4;\qquad \hat{\Omega}=\Omega T \quad (8)$$

Finally, (1) and (2) can be written as

ACCEPTED MANUSCRIPT

$$w_1''''(x_1,t)+\ddot{w}_1(x_1,t)+c_{non1}\dot{w}_1(x_1,t)=\frac{\alpha_1\left[V_{DC}+V_{AC}\cos(\Omega t)\right]^2}{(1-w_1+w_2)^2} \quad (9)$$

$$w_2''''(x_2,t)+\beta\ddot{w}_2(x_2,t)+c_{non2}\dot{w}_2(x_2,t)=\frac{-\alpha_2\left[V_{DC}+V_{AC}\cos(\Omega t)\right]^2}{(1-w_1+w_2)^2} \quad (10)$$

The normalized boundary conditions are

$$w_{1,2}(0,t)=0 \qquad \frac{\partial w_{1,2}}{\partial x_{1,2}}(0,t)=0$$

$$\frac{\partial^2 w_{1,2}}{\partial x_{1,2}^{\;2}}(1,t)=0 \qquad \frac{\partial^3 w_{1,2}}{\partial x_{1,2}^{\;3}}(1,t)=0 \quad (11)$$

Next, we solve the normalized system of equations (9) and (10) in conjunction with the boundary condition in (11) using the Galerkin approach [27]. Using this approach helps simplify the problem by reducing the partial differential equations into a system of coupled second-order differential equations (reduced-order model). Toward this, the deflections of the microbeams 1 and 2 are approximated as

$$w_1(x_1,t)=\sum_{i=1}^{n}u_i(t)\phi_i(x_1) \quad (12)$$

$$w_2(x_2,t)=\sum_{i=1}^{n}v_i(t)\phi_i(x_2) \quad (13)$$

where $\phi_i(x)$ are chosen as the ith undamped, unforced, linear, orthonormal modeshapes of the cantilever beam. Since the beams are almost of the same dimensions, the modeshapes of both beams are the same i.e. ϕ_i. Similarly u_i and v_i are the modal coordinates for respective beams, and n is the number of the assumed modes.

Note from Fig. 1(a) that

$$x_1=x_2+\delta \quad (14)$$

Hence

$$dx_1=dx_2 \quad (15)$$

In order to derive the reduced order model we substitute (12) and (13) in conjunction with (14) and (15) into (9) and (10), respectively. The outcome is then multiplied with the modeshapes ϕ_j and integrated over the beams spatial domains from 0 to 1.The final equations governing the system are then given by

$$\int_0^1\phi_j\left(\sum_{i=1}^{n}u_i(t)\phi_i''''(x_1)+\sum_{i=1}^{n}\ddot{u}_i(t)\phi_i(x_1)\right)dx_1+c_{non}\int_0^1\phi_j\left(\sum_{i=1}^{n}\dot{u}_i(t)\phi_i(x_1)\right)dx_1=\alpha_1\left[V_{DC}+V_{AC}\cos(\Omega t)\right]^2\int_0^1\left\{\frac{\phi_j}{\left(1-\sum_{i=1}^{n}u_i(t)\phi_i(x_1)+\sum_{i=1}^{n}v_i(t)\phi_i(x_2)\right)^2}\right\}dx_1 \quad (16)$$

$$\int_0^1\phi_j\left(\sum_{i=1}^{n}v_i(t)\phi_i''''(x_1)+\beta\sum_{i=1}^{n}\ddot{v}_i(t)\phi_i(x_1)\right)dx_1+c_{non}\int_0^1\phi_j\left(\sum_{i=1}^{n}\dot{v}_i(t)\phi_i(x_1)\right)dx_1=-\alpha_2\left[V_{DC}+V_{AC}\cos(\Omega t)\right]^2\int_0^1\left\{\frac{\phi_j}{\left(1-\sum_{i=1}^{n}u_i(t)\phi_i(x_1)+\sum_{i=1}^{n}v_i(t)\phi_i(x_1)\right)^2}\right\}dx_1 \quad (17)$$

Next, for the static simulations, all the time varying terms, including inertia, damping, and time varying forcing are set to zero in (16) and (17). Also, the time varying modal variables u_i are replaced by constant unknown coefficients C_i, and variables v_i are replaced by the constant unknown coefficients D_i. This reduces the system of equations (16) and (17) to the following set of nonlinear algebraic equations:

$$\int_0^1\phi_j\left(\sum_{i=1}^{n}C_i\phi_i''''(x_1)\right)dx_1=\alpha_1 V_{DC}^{\;2}\int_0^1\left\{\frac{\phi_j}{\left(1-\sum_{i=1}^{n}C_i\phi_i(x_1)+\sum_{i=1}^{n}D_i\phi_i(x_1)\right)^2}\right\}dx_1 \quad (18)$$

$$\int_0^1 \phi_j \left(\sum_{i=1}^{n} D_i \phi_i''''(x_1) \right) dx_1 = -\alpha_2 V_{DC}^2 \int_0^1 \left\{ \frac{\phi_j}{\left(1 - \sum_{i=1}^{n} C_i \phi_i(x_1) + \sum_{i=1}^{n} D_i \phi_i(x_1)\right)^2} \right\} dx_1 \quad (19)$$

In order to simplify the spatial integration of the forcing term [27], we multiply (16-19) by their denominators on both sides and the resulting system can be solved numerically using Runge-Kutta method [28] in case of (16) and (17) or using a Newton-Raphson method in the case of (18) and (19). The first three modeshapes for each equation show good convergence, and hence will be used to produce fairly the simulation results.

Next, we derive an analytical approximation for the static problem and the pull-in voltage for the special case of two identical beams. Fig. 4 shows the response of one of the beams against $\alpha_1 V_{DC}^2$ by solving (18) and (19) simultaneously.

It can be noted that the pull in occurs near $\alpha_1 V_{DC}^2 \approx 0.868$ which is universally true for beams of any dimensions as long as $\alpha_1 = \alpha_2$, i.e. beams are identical. Accordingly the pull-in voltage can be approximated as

$$V_{pull} = \sqrt{\frac{0.868}{\alpha_1}} \quad (20)$$

4. Experimental Setup

The static results are obtained by sweeping voltage against current using Keithley parameter analyzer. The device is mounted on a probe station in the air as shown in Fig. 5(a). The probes are then connected to the parameter analyzer inputs and outputs. In built software module of parameter analyzer is used to sweep voltage in small increments while monitoring the current. Large amount of current passes through the device indicating pull-in. The parameter analyzer then limits the current through device to avoid burning/stiction of the resonators. We also use the MSA-500 Polytec Micro System Analyzer for dynamic measurements, Fig. 5(b). The device is placed inside the vacuum chamber directly underneath the camera head of the Micro System Analyzer. The in-plane microstructure vibration and motion analysis is performed using stroboscopic video microscopy [29]. All the dynamic measurements are performed in low vacuum conditions i.e. 1-5 millitorr, with a quality factor of over 2000.

5. Results and discussion

5.1. Static Analysis

We start with exploring the static behavior of the device. The theoretical model developed in Section 3 is used to simulate the static characteristics of the system.

First, we consider the beams of case study 1 given in Table 1. We generate results for two arrangements. First, when the potential difference is applied in between the beams themselves, and the second when the beams are actuated against the fixed electrodes individually and separately (electrically uncoupled). Fig. 6 shows the simulated response of the voltage against the absolute displacement. It is worth mentioning here that the response plotted for the coupled dual beam case is the absolute sum of the distance covered by the two beams towards each other until they pull-in ($w_1 + w_2$). It is clear from the figure that $w_1 + w_2$ approaches the well-known displacement range of a single cantilever. Also it is noticed that the pull-in voltage for the dual beam is much lower.

Next, we demonstrate the pull-in value experimentally for the beam of case study 1. The response for all the different cases of actuation is shown in Fig. 7 in the form of an I-V plot.

Table 2 shows the pull-in values for case studies 1 and 2. The table shows the pull-in values for coupled beam actuation as well as single beam actuation against the respective fixed electrode.

It can be noticed from table 2 that, for case study 1 the pull-in value for the coupled beam actuation is 42% less than that of the pull-in value for the case when a single smaller beam with length 100 µm is actuated separately against the fixed electrode. Also, the coupled beam actuation pull-in value is 30.3% less than that of the pull-in value

ACCEPTED MANUSCRIPT

for the case when the larger beam with length 105 μm is actuated separately against the fixed electrode. In order to further clarify this, case study 2 analyzes the results when the beams are of same lengths. The beams of same length can be used as a standard for analyzing electrostatically coupled dual beam resonators. This case study shows that the pull-in value in the case of the coupled beam actuation is almost 36% less than that of the pull-in value in the case of a single beam actuation. This shows that, there is a significant decrease in the pull-in value in the case of actuation of the two beams among themselves as compared to the actuation of the beams separately with respect to the fixed electrodes. One can note that using (20), the pull-in voltage of the dual case is found to be 80.5 V, which is close to the numerically calculated value in Table 2.

Next, we study the response of each of the two beams separately against the applied voltage for the case of coupled beam actuation. Fig. 8 shows such response for case study 1 and 2.

Fig. 8(a) shows that the larger beam travels about 24% of the distance while the smaller beam travels about 20% of the distance towards each other before they pull-in. This is due to the fact that the larger beam is less stiff and hence bends more, while the smaller beam is stiffer and hence bends less. Also, we notice that the sum of the distance traveled by the two beams towards each other is 44% of the total gap between the beams. This value is the same as the value of distance traveled by a cantilever towards a fixed electrode before pull-in [27]. Also from Fig. 8(b), we notice that the distance traveled by the two beams towards each other is exactly the same since the beams are of same dimensions. The sum of these distances is 44% as expected. This characteristic of the electrostatically coupled dual beam resonators is promising in applications where lower pull-in voltages are required. It also allows for less distance traveled by each beam before it pulls in, which might be useful in applications, where abrupt sensing and actuation is required.

The reduction in pull-in value depends on the length of the beam that replaces the fixed electrode. A standard reduction in pull-in value of 36% percent will occur if the two beams are of exact same dimensions. However, a greater reduction in pull-in value of a stiffer beam can also be achieved if the stiffer beam is actuated next to a beam with much less stiffness. This is due to the fact that, we can make the less stiff beam travel most of the distance towards the stiffer beam at a much less voltage value and cause pull-in. This also shows that by varying the lengths of the beams, we can also control the distance traveled by each beam before it pulls in. These characteristics of electrostatically coupled dual beam resonators provide greater tunability and control over the pull-in characteristics of microbeams, which exhibit great promise in switching and sensing applications.

Next, we investigate the impact of the electrostatic coupling on the pull-in time. Pull-in time is defined as the time the microbeam requires to hit the other electrode during the pull-in event. In the case of a single beam actuation, this means the time it takes the beam to travel the complete gap distance (w_{max}/d=1). In the case of two identical beams, this means the time it takes for one of the beams to travel half the width of the gap, w_{max}/d=0.5 (where they hit and contact each other during the pull-in event). We simulate the response for the beams of case study 2. The time history response for this case is shown in Fig. 9. We notice here that the pull-in time for single beam actuation and coupled beam actuation is almost the same for their respective values of pull-in i.e. 123.4 volts and 78.9 volts respectively. This may be due to the fact that the pull-in voltage value is different in both the cases. However, if we take the pull-in value for the case of the single beam actuation against the fixed electrode i.e. 123.4 volts and apply it among the two beams themselves; we find that the pull-in time is reduced by the 38.46%.

Next, the shift in the natural frequency against V_{DC} for case study 2 is explored and plotted in Fig. 10. These results are obtained by solving the eigenvalue problem of the reduced-order model, linearized around the static deflection due to the DC voltage [27]. It is observed that a higher frequency shift can be achieved at a much smaller voltage when the fixed electrode is replaced by a similar cantilever. This is another characteristic that could be useful in sensing applications that rely on frequency shifts [1-3].

5.2. Dynamic Analysis

Here we compare the results of individual uncoupled beam actuation against the fixed electrode with the case of coupled beam actuation among the two beams. We plot the theoretical as well as the experimental frequency response curves of the beams from under DC plus AC harmonic loading. First we consider case study 1. The plots are shown in Fig. 11.

ACCEPTED MANUSCRIPT

The first observation that can be made here is that the response in the case of the coupled beam arrangement for the longer beam is slightly higher than the case when the beam is individually actuated, Fig. 11(a). The is due to the fact that both beams are now moving towards each other as a result of coupling and the electrostatic force between the beams is higher as compared to the case of a single beam actuated against a fixed electrode. We also notice from Fig. 11 that the response of the longer beam in the coupled actuation is higher compared to the response of the shorter beam, which is expected since the stiffness is different in both the cases with the longer beam being less stiff. Hence, we conclude that the response of the beams in case of coupled actuation arrangement is slightly higher for the longer beam and slightly lower for the stiffer beam compared to the case of these beams actuated individually against their respective fixed electrode. Finally, it is also observed that the frequency shift in case of coupled beam arrangement is slightly greater than in case of single beam actuation against the fixed electrode. We also observe from the results of Fig. 11 that the theoretical model predicts the experimental results with acceptable accuracy.

Next, we investigate the effect of coupling on the dynamics of nearly identical beams, as we actuate the beams of case study 3 by applying potential difference among them. Fig. 12 shows the frequency response plots for this case.

First, we observe from Fig. 12 that, the coupled system shows two resonance frequencies associated with each beam. It is observed that when one of the beams is vibrating at its resonance frequency, the other beam also shows slightly higher amplitude at that specific frequency as a result of electrostatic coupling. We can also notice that the longer beam being less stiff is affected more by the coupling compared to the smaller beam. In order to further investigate this, we study how we can increase the effect of one beam on the other by strengthening the coupling between them. Toward this, we increase the value of DC voltage significantly while applying lower AC voltages in order to avoid pull-in. Fig. 13 shows the simulated and measured response of the coupled beam system of case study 3 under variable actuation voltages.

It is observed that the electrostatic coupling between the two beams increases significantly as the DC voltage is increased, which is expected. It is also noticed that the longer beam shows softening behavior near its natural frequency and induces softening behaviour in the other beam at this frequency as well. However, the stiffer beam stays inside the linear regime only, even after application of large voltages. The analysis of the dynamic characteristics of the dual beam resonators show that we can control the electrostatic coupling among the dual beam resonators easily by manipulating the input voltages. It is observed from Fig. 13 that the nonlinearity is triggered in the beams at a much less amplitude. It also shows that we can have a resonator where the linear and nonlinear regimes coexist at slightly apart frequencies at the same time, Fig. 13(c)/(d). This could be useful for applications in MEMS sensing. We also notice that the coupled beam resonators can be used to increase the bandwidth of the resonator by actuating two nearly identical resonators as shown in Fig. 12.

The effect of V_{DC} on electrsoatic coupling and how it gets stronger with increasing V_{DC} can be better understood by looking at the modeshapes of the dual beams at their resonant modes. We perform finite element analysis on the beams of case study 3 in air to demonstrate this effect. Fig. 14 shows the first two modeshapes of the coupled system under different DC voltages.

We notice from Figs. 14 (a) and (b) that under the influence of almost negligible DC voltage, i.e., 1V, the two beams move independently and no modeshape coupling is observed. However as increasing the DC voltage we start to see the global modeshapes appear. Figs. 14 (b) and (c) indicate that under V_{DC} =40V, the first modeshape shows the two beams moving out of phase from each other, whereas in Figs. 14 (a) and (b) one beam moves while the other beam remains almost stationary. Similarly the second modeshape shows the two beams moving in phase. As we further increase the DC voltage among the beams, the global nature of the modeshapes become more apparent and are very evident in Fig. 14 (e) and (f). These results of Fig. 14 are in line with the reported experimental data and simulation results in Fig. 13, where increasing the DC voltage has been demonstrated to significantly affect the emergence and strength of the coupled-mode resonances.

Finally, the dynamic pull-in of the coupled dual beam system is studied experimentally by studying the response of two nearly identical beams of case study 3. Fig. 15 shows the response of the beams.

It is noticed that under higher voltages the coupled beams experience pull-in. It is clear that pull-in bands are reported near the resonance frequencies of both of the beams [30, 31]. Therefore, the coupled system exhibits two pull-in bands fairly close to each other separated by a stable region in between. This stable region in between can be

ACCEPTED MANUSCRIPT

shrunk depending on the closeness of the frequencies of the two beams and by applying the appropriate voltages, Fig. 15. Operating on this small region in between gives us the liberty to pull-in by either an increase or a decrease in the resonance frequency. This feature of the coupled beams is again very interesting for sensors depending on the frequency shift and provides an opportunity to sense a positive or negative frequency shift.

Next, we consider the 140 μm beam near its pull-in band in Fig. 15. It can be observed that the amplitude of the beam gradually increases as it approaches the resonance frequency and eventually pulls in. However, at the same time the induced motion in the 139 μm beams stays almost negligible while the 140 μm approaches the resonance frequency and suddenly pulls in when the 140 μm beam pulls in. This shows that depending on the beam under observation, we can have a sudden pull-in from almost negligible amplitude as well as experience an increase in amplitude before eventually the beams pull-in. This phenomenon happens at the resonance frequencies of both of the beams.

6. Conclusions

The static and dynamic characteristics of the electrostatically coupled and laterally actuated dual beam resonators are studied theoretically and experimentally. The dual beam resonators are demonstrated as a way to reduce the pull-in voltage as well as pull-in time by more than 30% as compared to the case of individual beam actuation against the fixed electrode. A great extent of control is exhibited over the amount of pull-in voltage that can be reduced and also the motion of each beam before they pull-in. These characteristics are considered valuable in applications where lower pull-in voltages and fast switching speeds are necessary. The dynamics of the dual beam resonators are also explored via frequency response plots near the neighborhood of natural frequency. The results show that we can control the coupling between the resonators by manipulating the DC voltage. It is also noticed the motion of one beam at its natural frequency influences the motion of other beam at that frequency and the influence intensifies as the coupling grows stronger. Based on these characteristics of the electrostatically coupled dual beam resonators, they are also proposed as a way to increase bandwidth near the natural frequency of the beam. Finally, dynamic pull-in of the coupled system is studied and proposed as sensor capable of sensing both a positive or negative shift in the frequency.

ACKNOWLEDGMENT

This work has been supported through King Abdullah University of Science and Technology (KAUST) research funds.

REFERENCES

[1] R. Bogue, "Mems sensors: past, present and future", *Sensor Review*, vol. 27, no. 1, pp. 7-13, 2007.

[2] M. Li , H. X. Tang and M. L. Roukes "Ultra-sensitive NEMS-based cantilevers for sensing, scanned probe and very high-frequency applications", *Nat. Nano.*, vol. 2, pp.114 -120, 2007.

ACCEPTED MANUSCRIPT

[3] Y. T. Yang , C. Callegari , X. L. Feng , K. L. Ekinci and M. L. Roukes "Zeptogram-scale nanomechanical mass sensing", *Nano Lett.,* vol. 6, no. 4, pp.583 -586, 2006.

[4] A. K. Sharma and N. Gupta", Microelectromechanical System (MEMS) Switches for Radio Frequency Applications-A Review", *Sens. Transducers*, vol. 148, pp. 11-21, 2013.

[5] C. T.-C. Nguyen, "Rf mems in wireless architectures," *Proc. of DAC '05*, pp. 416-420, 2005.

[6] H. M. Ouakad and M. I. Younis, "On using the dynamic snap-through motion of MEMS initially curved microbeams for filtering applications," *J. Sound Vib.*, vol. 333, no. 2, pp. 555-568, 2014.

[7] S. Ilyas, A. Ramini, A. Arevalo, andM.Younis, “An Experimental and Theoretical Investigation of a Micromirror Under Mixed-Frequency Excitation.”, *J. Microelectromech. Syst.,* vol. 24, no. 4, pp. 1124 -1131, 2015.

[8] X. C. Zhang, E. B. Myers, J. E. Sader, and M. L. Roukes, "Nanomechanical Torsional Resonators for Frequency-Shift Infrared Thermal Sensing", *Nano Lett.,* vol. 13, pp. 1528-1534, 2013.

[9] S. Ilyas, A. Arevalo, E. Bayes, I.G. Foulds and M. Younis, "Torsion based universal MEMS logic device," *Sensor. Actuat. A-Phys*, vol. 236, pp. 150-158, 2015.

[10] D.I Caruntu, and K. N Taylor, “Reduced Order Model of Two Coupled MEMS Parallel Cantilever Resonators Under DC and AC Voltage Near Natural Frequency”. *ASME Int. Mech. Eng Con. Exp*, pp. 395-400, Nov. 2012.

[11] B K. Hammad, “Natural Frequencies and Mode Shapes of Mechanically Coupled Microbeam Resonators with an Application to Micromechanical Filters,” *Shock. Vib.*, vol. 2014,. doi:10.1155/2014/939467.

[12] M. Napoli , W. Zhang , K. Turner and B. Bamieh "Characterization of electrostatically coupled microcantilevers", *J. Microelectromech. Syst.*, vol. 14, no. 2, pp. 295 -304, 2005.

[13] Y. Lin, W.-C. Li, I. Gurin, S.-S. Li, Y.-W. Lin, Z. Ren, B. Kim, and C. T.-C. Nguyen, “Digitally-specified micromechanical displacement amplifiers,” Proc. *Transducers*, pp. 781–784, 2009.

[14] M. M. Shalaby, M. A. Abdel moneum, and K. Saitou, “Design of spring coupling for high-Q high-frequency MEMS filters for wireless application,” *IEEE Trans. Ind. Electron.*, vol. 56, no. 4, pp. 1022–1030, Apr. 2009.

[15] F. D. Bannon, III, J. R. Clark, and C. T.-C. Nguyen, “High-*Q*HF micromechanical filters”, *IEEE J. Solid-State Circuits*, vol. 35, pp.512 -526, 2000.

[16] P. Siavash, and F. Ayazi. "Electrically coupled MEMS bandpass filters: Part I: With coupling element." *Sensor. Actuat. A-Phys*, vol. 122, pp. 307-316, 2005.

[17] P.Siavash, and F. Ayazi. "Electrically coupled MEMS bandpass filters: Part II. Without coupling element." *Sensor. Actuat. A-Phys*, vol. 122, pp. 317-325, 2005.

[18] M.-H. Li, C.-Y. Chen, W.-C. Chen, and S.-S. Li, "A vertically coupled MEMS resonator pair for oscillator applications," *J. Microelectromech. Syst*., vol. 24, no. 3, pp. 528-530, Jun. 2015. DOI: 10.1109/JMEMS.2015.2421555.

[19] C. Y. Chen, M. H. Li, C. H. Chin, C. S. Li, and S. S. Li, “Combined electrical and mechanical coupling for mode-reconfigurable CMOS-MEMS filters.” *Proc. 27th IEEE Int. Conf. Micro Electro Mech. Syst*, pp. 1249-1252, Jan, 2014.

[20] M.-H. Li, W.-C. Chen, and S.-S. Li, "Mechanically-coupled CMOS-MEMS free-free beam resonator arrays with enhanced power handling capability*", IEEE Tran. Ultrasonics, Ferroelectrics, and Frequency Control*, vol. 59, no. 3, pp. 346-357, March 2012.

[21] P. Belardinelli, S. Lenci, and L. Demeio. "Vibration frequency analysis of an electrically-actuated microbeam resonator accounting for thermoelastic coupling effects." *Int. J. Dyn. Control,* vol 3, no. 2, pp.157-172, 2014.

[22] H. Samaali, F. Najar, S. Choura, A.H. Nayfeh, M. Masmoudi, “A double microbeam MEMS ohmic switch for RF-applications with low actuation voltage,” *Nonlinear Dyn,* vol 63, pp. 719–734, 2011.

[23] Y. Wang , Z. Li , D. T. McCormick and N. Tien, “A low voltage lateral MEMS switch with high RF performance”, *J. Microelectromech. Syst.*, vol. 13, no. 6, pp.902 -911, 2004.

[24] N. Sinha , Z. Guo , A. Tazzoli , A. DeHon and G. Piazza "1 volt digital logic circuits realized by stress-resilient ALN parallel dual-beam MEMS relays", *Proc. IEEE 25th Int. Conf. Micro Electro Mech. Syst*., pp.668 -671, 2012.

[25] M. Daneshmand , D. Yan and R. Mansour., "Thermally actuated multiport RF MEMS switches and their performance in a vacuumed environment", *IEEE Trans. Microw. Theory Tech.,* vol. 55, no. 6, pp.1229 -1236, 2007.

[26] M.W., Kim, Y.H. Song, S.D Ko, S.J. Ahn, and J.B. Yoon. "Ultra-low voltage MEMS switch using a folded hinge structure." *Micro. Nano. Syst. Let,*.vol 2, no. 1, pp. 1-5, 2014.

[27] M. I. Younis, *MEMS Linear and Nonlinear Statics and Dynamics:* Springer, New York, 2011.

[28] J. C. Butcher, *The numerical analysis of ordinary differential equations: Runge-Kutta and general linear methods*: Wiley-Interscience, Michigan, 1987.

[29] **Polytech: http://www.polytec.com/us/.**

ACCEPTED MANUSCRIPT

[30] F. Alsaleem, M. I. Younis, and H. Ouakad, "On the Nonlinear Resonances and Dynamic Pull-in of Electrostatically Actuated Resonators," *J. Micromech. Microeng*, Vol., 19, Article ID 045013, 14 pages, 2009.
[31] Alsaleem, F. M., Younis, M. I, and L. Ruzziconi, "An Experimental and Theoretical Investigation of Dynamic Pull-in in MEMS Resonators Actuated Electrostatically," *J. Microelectromech. Syst.*, Vol. 19, Issue 4, pp. 794 - 806, 2010.

ACCEPTED MANUSCRIPT

Saad Ilyas received a B.S. degree in Mechanical Engineering from Ghulam Ishaq Khan Institute of Engineering Sciences and Technology, Pakistan in 2012. He started his Masters in Mechanical Engineering from King Abdullah University of Science and Technology (KAUST) in 2013 and completed in 2014. He is currently enrolled as a PhD student in Mechanical Engineering in KAUST. His research interests include linear and nonlinear dynamics of MEMS devices with applications in MEMS sensors and actuators. He is a student member of American Society of Mechanical Engineers (ASME).

Karumbaiah N. Chappanda, PhD, was awarded a Bachelor of Engineering degree in Electronics and Communications from the Visvesvaraya Technological University in 2007, MS degree in Electrical Engineering from the Michigan Technological University in 2010, and PhD degree in Electrical Engineering from University of Utah in 2013. He is currently working as a post doctoral fellow in King Abdullah University of Science Technology, Physical Science and Engineering Division. His current research interest involves fabrication and characterization of micro and nano resonators. He is author and co-author of over 14 publications in peer-reviewed journals and conference proceedings.

Md. Abdullah Al Hafiz received his B.Sc. (Engg) degree in Electrical and Electronic Engineering from the Islamic University of Technology (IUT), Dhaka, Bangladesh, in 2001. From April 2003 to February 2006, he was a lecturer in the Department of EEE at the Rajshahi University of Engineering and Technology (RUET), Rajshahi, Bangladesh. In February 2011, he received his Ph.D. degree in Electrical Engineering from the University of New South Wales (UNSW), Sydney, Australia. Currently, he is working as Post-doc Fellow at KAUST in the area of using MEMS resonators for tunability and for logic and memory applications. His research interests are MEMS/MOEMS systems, planar light wave technologies, interconnects, optical cross-connects, and MEMS resonators.

ACCEPTED MANUSCRIPT

Mohammad I. Younis received the B.S. degree in mechanical engineering from the Jordan University of Science and Technology, Irbid, Jordan, in 1999, and the M.S. and Ph.D. degrees in engineering mechanics from Virginia Polytechnic Institute and State University, Blacksburg, VA, USA, in 2001 and 2004, respectively. He is currently an Associate Professor of Mechanical Engineering with the King Abdullah University of Science and Technology, Thuwal, Saudi Arabia, and the State University of New York (SUNY), Binghamton, NY, USA. He serves as the Director of the MEMS and NEMS Characterization and Motion Laboratory. Dr. Younis is a recipient of the SUNY Chancellor's Award for Excellence in Scholarship and Creative Activities in 2012, the National Science Foundation Faculty Early Career Development Award in 2009, and the Paul E. Torgersen Graduate Research Excellence Award in 2002. He holds several U.S. patents in MEMS sensors and actuators. He serves as an Associate Editor of Nonlinear Dynamics, the Journal of Computational and Nonlinear Dynamics, the Journal of Vibration and Control, and Mathematical Problems in Engineering. He has authored the book entitled MEMS Linear

and Nonlinear Statics and Dynamics (Springer, 2011). He is a member of the American Society of Mechanical Engineers.

ACCEPTED MANUSCRIPT

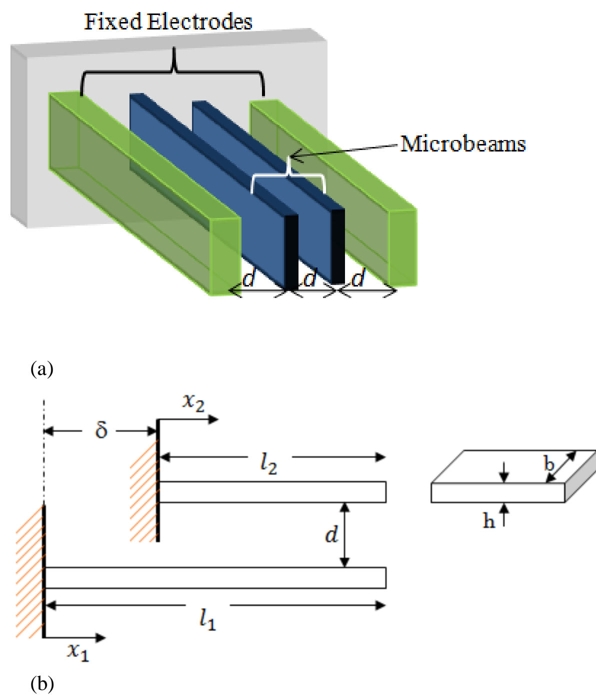

Fig.1. Schematics of the laterally electrostatically actuated and coupled resonators. (a) 3D view. (b) 2D side view.

ACCEPTED MANUSCRIPT

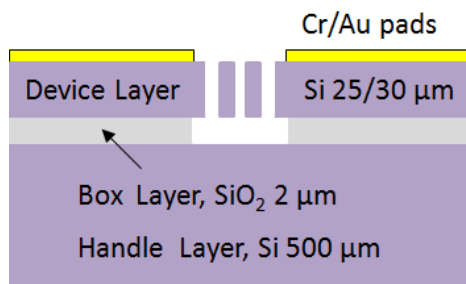

Fig.2. Cross section of the electrostatically coupled beam resonators.

ACCEPTED MANUSCRIPT

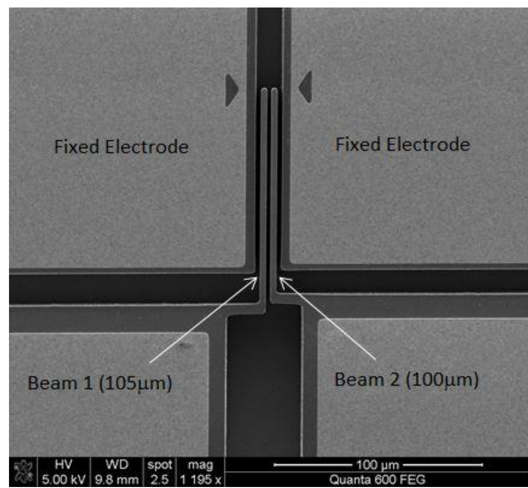

Fig.3. A SEM image of the fabricated electrostatically coupled beam resonators.

ACCEPTED MANUSCRIPT

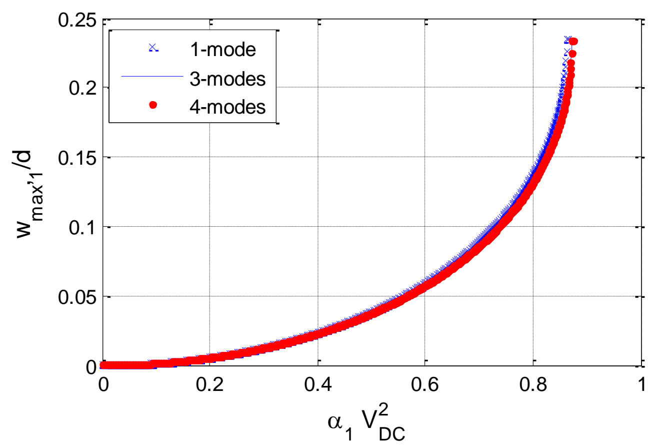

Fig.4. Response of the dual beam resonators against applied voltage for different modes.

ACCEPTED MANUSCRIPT

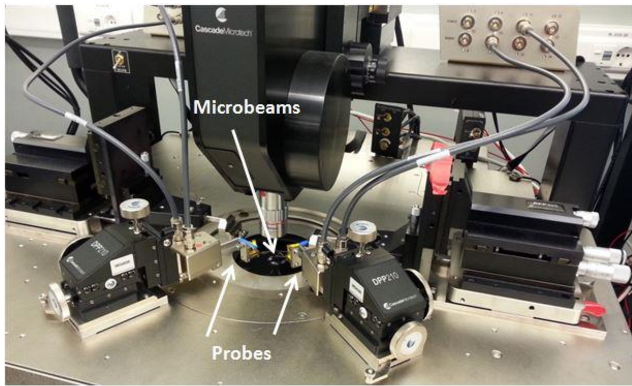

(a)

(b)

Fig.5. Experimental setup for the characterization of coupled beam resonators. (a) Probe station (b) Micro System Analyzer.

ACCEPTED MANUSCRIPT

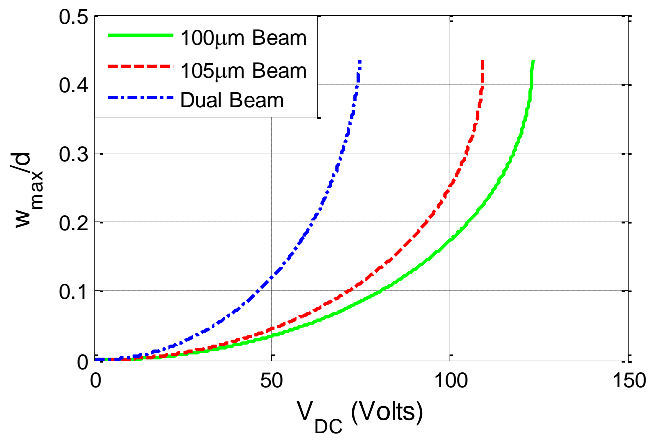

Fig.6. Simulated response of the beams of case study 1 demonstrating pull-in voltages for different cases of actuation.

ACCEPTED MANUSCRIPT

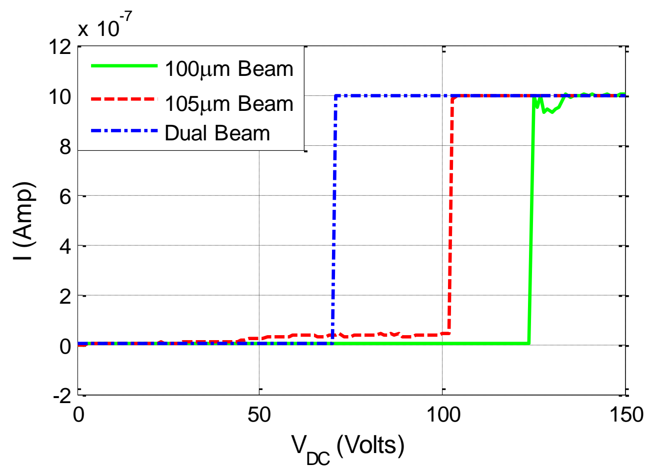

Fig.7. Experimentally measured pull-in voltages for different cases of actuation for the beams of case study 1.

ACCEPTED MANUSCRIPT

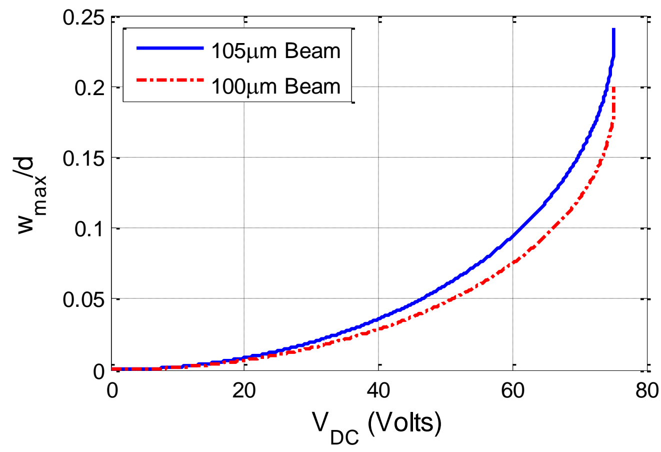

(a)

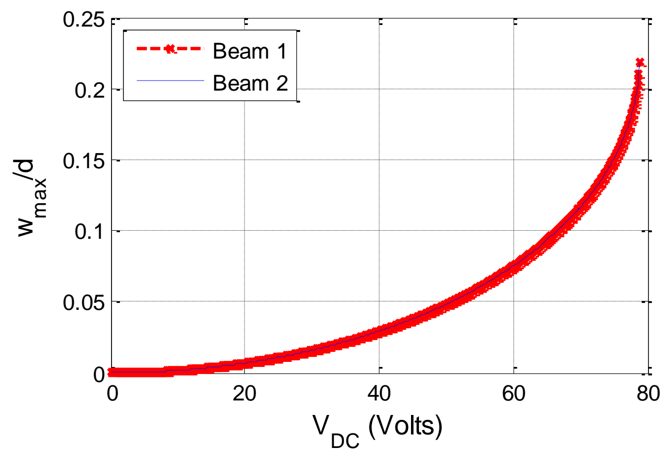

(b)

Fig.8. Simulated response of each of the coupled beams against the applied DC voltage for (a) case study 1 (b) case study 2.

ACCEPTED MANUSCRIPT

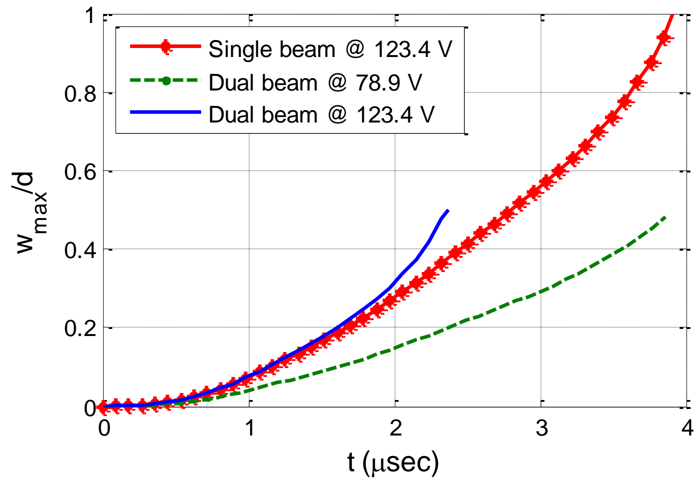

Fig.9. Simulated time response for beams of case study 2 demonstrating pull-in time under different actuation conditions.

ACCEPTED MANUSCRIPT

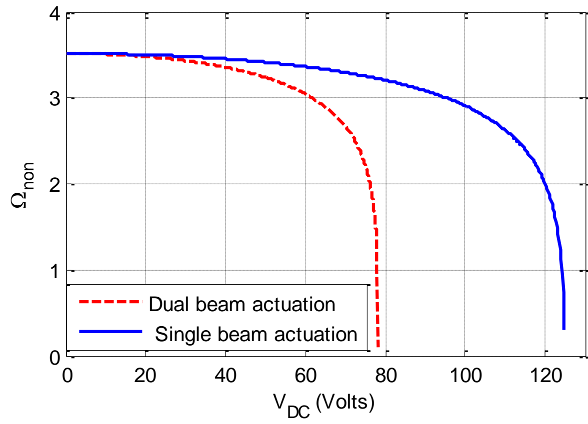

Fig.10. Simulated natural frequency shift against V_{DC} for coupled resonators of case study 2.

ACCEPTED MANUSCRIPT

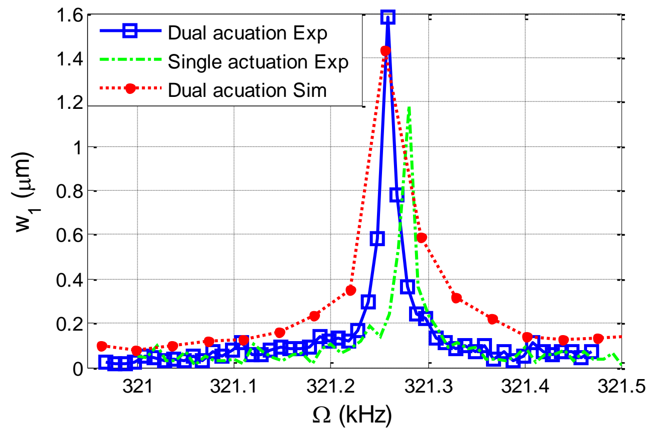

(a)

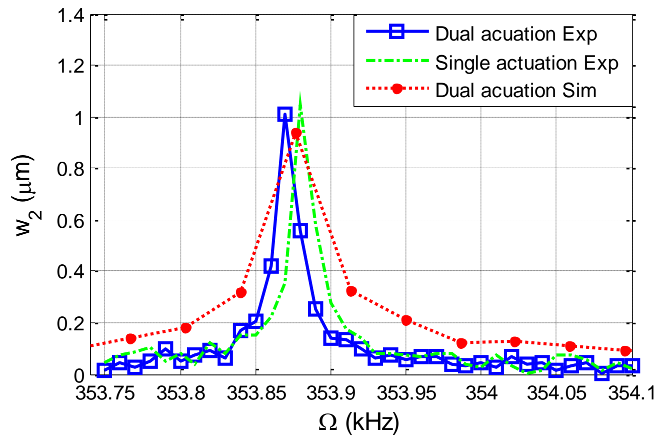

(b)

Fig.11. Frequency response of the beams of case study 1 under V_{DC} =1.5 V, V_{AC} =300 mV for (a) 105 µm beam, (b) 100 µm beam.

ACCEPTED MANUSCRIPT

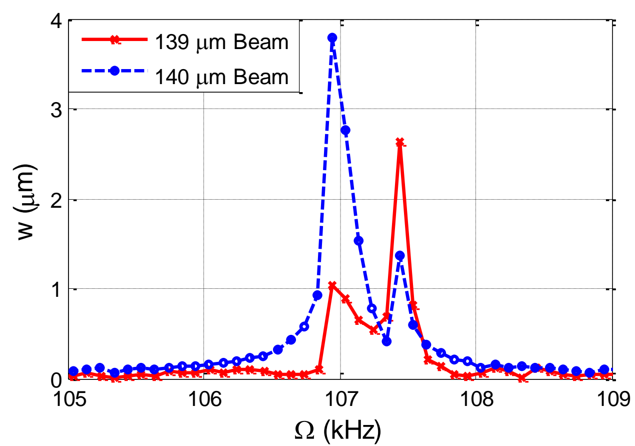

Fig.12. Frequency response of the beams of case study 3under V_{DC} =3 V, V_{AC} =3 V.

ACCEPTED MANUSCRIPT

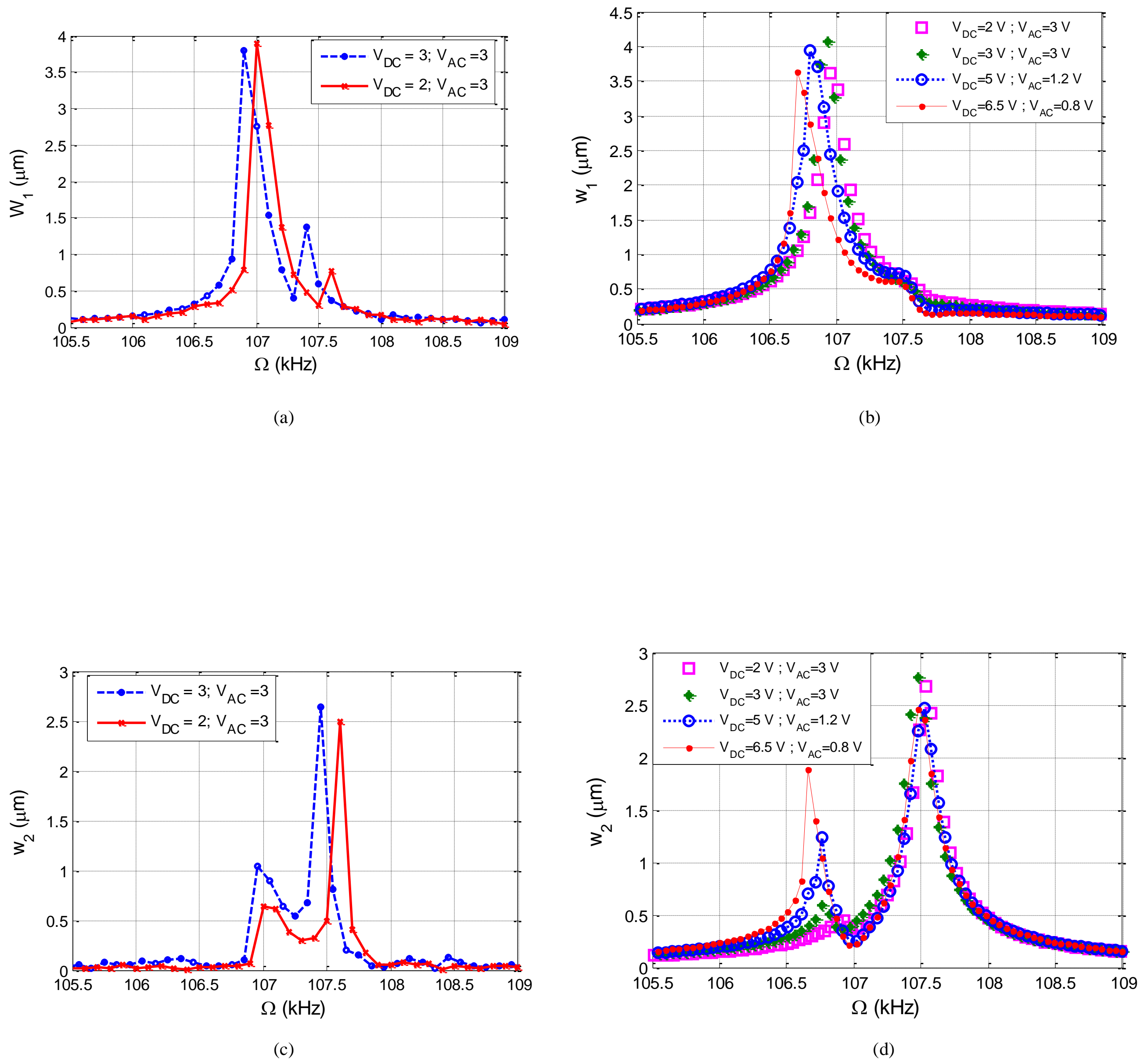

Fig.13. Frequency response of the beams of case study 3 under various actuation voltages. (a) Experimental and (b) simulated response for 140 μm long beam. (c) Experimental and (d) simulated response for 139 μm long beam.

ACCEPTED MANUSCRIPT

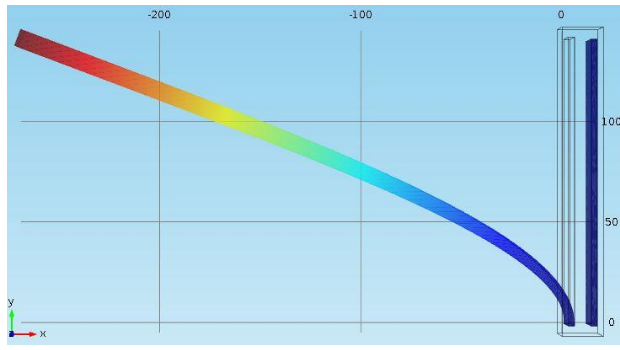

(a)

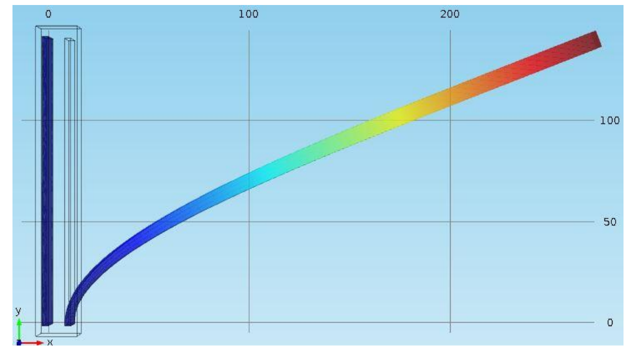

(b)

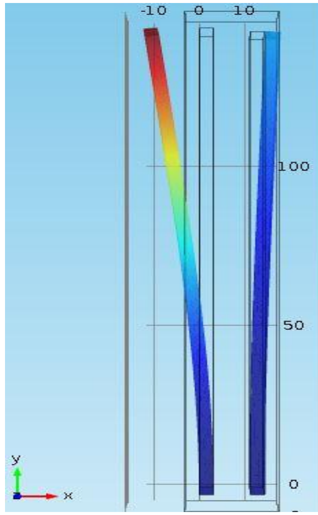

(c)

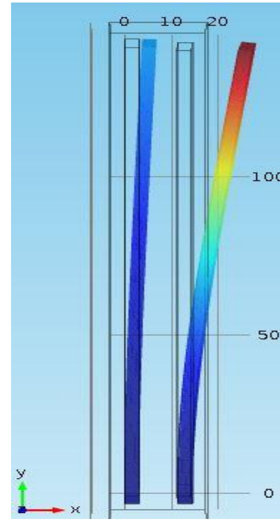

(d)

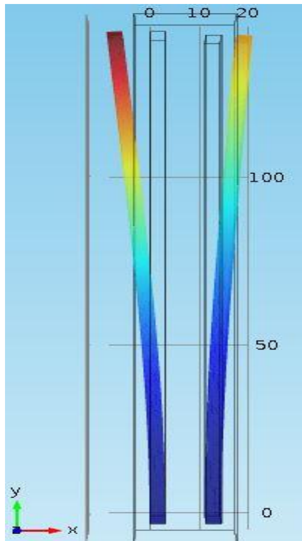

(e)

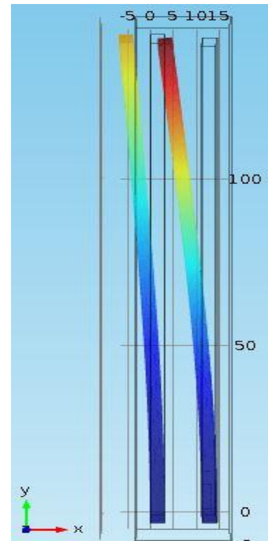

(f)

Fig.14. FEM simulations of modeshapes of the dual beam system of case study 3 under various DC voltages. (a) 1st modeshape and (b) 2nd modeshape under V_{DC}=1V. (c) 1st modeshape and (d) 2nd modeshape under V_{DC}=40V. (e) 1st modeshape and (f) 2nd modeshape under V_{DC}=70V.

ACCEPTED MANUSCRIPT

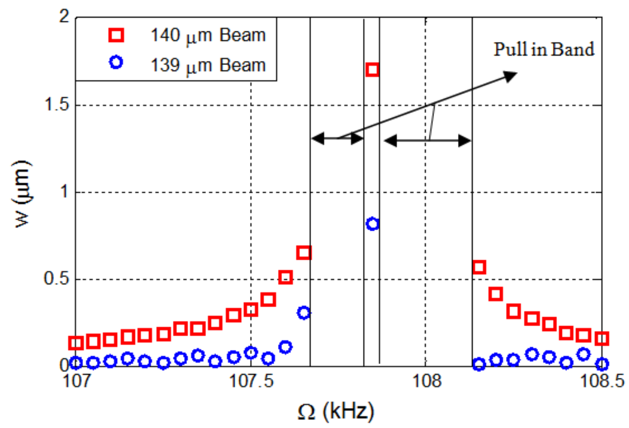

Fig.15. Frequency response of the beams of case study 3 under V_{DC} =10 V, V_{AC} =10 for the dual beam actuation. The plot shows the pull-in bands observed in the coupled system.

ACCEPTED MANUSCRIPT

Table 1 summarizes the dimensions and other important parameters of the different case studies under consideration.

Table1

Specifications of the microbeams for the three case studies under consideration.

Case study 1	Length of beam 1	l_1	105µm
	Length of beam 2	l_2	100µm
	Height of the beam	b	25µm
	Thickness of the beam	h	3µm
	Gap	d	2µm
Case study 2	Length of beam 1	l_1	100µm
	Length of beam 2	l_2	100µm
	Height of the beam	b	25µm
	Thickness of the beam	h	3µm
	Gap	d	2µm
Case study 3	Length of beam 1	l_1	140µm
	Length of beam 2	l_2	139µm
	Height of the beam	b	30µm
	Thickness of the beam	h	3µm
	Gap	d	8µm

ACCEPTED MANUSCRIPT

Table 2
Pull-in values for different case studies under different cases of actuation.

Case study		Experimental Pull-in Value	Theoretical Pull-in Value
1	100 µm beam	124 Volts	123.4 Volts
	105 µm beam	103 Volts	109.5 Volts
	Coupled actuation	71 Volts	74.9 Volts
2	100 µm beam		123.4 Volts
	Coupled actuation		78.9 Volts